

ABSTRACT

Simulation and Optimization of the HINS Ion Source Extraction System

Eugene S. Evans (University of California-Berkeley, Berkeley, CA 94720), Raymond Tomlin (Fermi National Accelerator Laboratory, Batavia, IL 60510).

The heart of the High Intensity Neutrino Source (HINS) linear accelerator (linac) is a magnetron-type, circular aperture H^- source, which is currently being tested at Fermilab. Although this prototype already delivers the beam current and emittance required by the HINS project, an exploration of whether or not the performance of the source could be improved was undertaken. To this end, the extraction geometry of the source was simulated with SIMION 8.0 and Finite Element Method Magnetics. The effects of changing the angle of the extraction cone (cone angle), the size of the gap between the extraction cone and the source plate (extraction gap), and the aperture of the extraction cone (extraction aperture) were studied. These parameters were chosen because we thought that they would have the greatest impact on space charge effects, which is a major source of emittance growth in this ion source. Based on the results of these simulations, four different configurations were ultimately tested in the ion source. The simulations indicated that the final emittance of the source should be significantly decreased by utilizing geometry with a 45 degree cone angle, a 4 mm extraction gap, and a 3 mm extraction aperture. Subsequent emittance measurements on the ion source have confirmed this result. This new geometry also allows the source to output a higher current beam with the same duty factor.

1 Introduction

The High Intensity Neutrino Source (HINS) linear accelerator (linac) is a proposed superconducting linear accelerator ultimately intended for the production of high-intensity neutrino beams. First proposed in 2005, the HINS R&D program comprises contributions from Fermilab, Argonne National Laboratory, Lawrence Berkeley National Laboratory, Brookhaven National Laboratory and the Oak Ridge Spallation Neutron Source. Fermilab houses the accelerator at its Meson Detector Building, which contains at present a duoplasmatron proton source and associated optics for injection into a 2.5 MeV RFQ [Fig. 10]. The front end of this linac, from the RFQ to the first major superconducting cavity, is powered by one 325 MHz klystron. The proton source will be replaced with an H^- source, which is currently under development in the HINS ion source testbed [1].

2 Background

2.1 The HINS Ion Source

The HINS H^- ion source is being tested on the linac ion source testbed [Fig. 7]. It is a magnetron surface-plasma source similar to the magnetron sources presently used at Fermilab. The source features a circular aperture in the anode and corresponding round dimple in the cathode to produce a round beam. For good operation of magnetron sources, cesium is added to the plasma so as to reduce the work function of the cathode from 4.5 eV to 2 eV or less. Figure 8 shows the basic parts of a magnetron source. Collisions between plasma ions and the cathode liberate electrons as well as hydrogen ions. A magnetic field parallel to the axis of the cathode confines the electrons to the plasma for a relatively long time, while some of the hydrogen atoms are transformed into H^- ions by electron capture through collisions with the cathode. The ions then travel through the 1 mm wide plasma and are extracted at the aperture of the source.

A diagram of the interior of the source is shown in Figure 7b. The source box itself is held at -50 kV, with two electrodes at the output to extract and accelerate the ions. Both electrodes have a cone-shaped geometry near the beam axis, with the tip pointed toward the source, so as to minimize sparking in the gaps. Downstream, the beam passes through an electrostatic lens to focus the beam onto a Faraday collector for beam current measurement; a current toroid located after the lens provides another diagnostic of the beam current. A quartz window can be rotated into the beamline to help visualize the beam, and horizontal and vertical scanners are used to characterize the emittance. Initially, the tip of the extraction electrode was located 2 mm from the source plate (gap), with an aperture of 2 mm (aperture) and an angle of 30 degrees relative to the beam axis (cone angle), and had a voltage (relative to the source potential) of 12 kV to 14 kV (extraction voltage). This configuration produced approximately 21 mA of H⁻, with a duty factor of $\approx 0.25\%$ (1 ms pulse at 2.5 Hz repetition rate).

2.2 Emittance

A beam of particles can be characterized by its emittance, a measure of the beam in phase space. Several definitions exist; in the most general terms, emittance is the volume occupied by a beam in the six-dimensional phase space, $dx dy dz dp_x dp_y dp_z$ [6]. Assuming the particles move relatively independently in the transverse and longitudinal directions, it is acceptable to consider the transverse and longitudinal emittances separately. Further, if the motions of the particles in the transverse directions are independent, then the transverse emittances (in x and y directions) can also be considered separately. For beams of sufficient energy, the paraxial approximation ($\sin\theta \approx \theta$) can be made, so that the velocities of the beam particles can be used in place of their momenta [5]. Finally, in order to compare beams of different energies, the emittance is normalized by the relativistic factor $\beta\gamma$. Then, the transverse emittances of such a beam are given by equation 1.

$$\varepsilon_{x,norm} = \beta\gamma \int \int dx dx', \quad \varepsilon_{y,norm} = \beta\gamma \int \int dy dy' \quad (1)$$

A variety of methods exist for calculating emittances from real and simulated data. The normalized rms emittance, given here for (x, x') [Zhang], is convenient to use as a means of comparing the outcome of the various simulations that follow. In the actual calculations, the intensity distribution in phase space, $c(x, x')$, is set to 1 since the simulations use low numbers of discrete particles.

$$\begin{aligned} \varepsilon_{rms,norm} &= \beta\gamma \sqrt{\langle x^2 \rangle \cdot \langle x'^2 \rangle - \langle x \cdot x' \rangle}; & \langle x^2 \rangle &= \frac{\Sigma_{all} (x - \bar{x})^2 \cdot c(x, x')}{\Sigma_{all} c(x, x')}, & \bar{x} &= \frac{\Sigma_{all} x \cdot c(x, x')}{\Sigma_{all} c(x, x')}, \\ \langle x'^2 \rangle &= \frac{\Sigma_{all} (x' - \bar{x}')^2 \cdot c(x, x')}{\Sigma_{all} c(x, x')}, & \bar{x}' &= \frac{\Sigma_{all} x' \cdot c(x, x')}{\Sigma_{all} c(x, x')}, & \langle x \cdot x' \rangle &= \frac{\Sigma_{all} (x - \bar{x}) \cdot (x' - \bar{x}') \cdot c(x, x')}{\Sigma_{all} c(x, x')} \end{aligned} \quad (2)$$

An ideal beam has a zero emittance; all physical beams have a finite, nonzero emittance [Fig. 11]. Liouville's theorem guarantees that emittance is invariant in the presence of conservative forces (like external electromagnetic fields), making this a useful quantity when analyzing the behavior of a particle beam as it passes through various beamline elements. A variety of nonconservative forces, notably space charge, cause emittance to increase; on the other hand, transverse emittance decreases as beam energy increases, and space charge effects decrease with beam energy due to special relativity. Therefore, it is desirable to accelerate a beam as quickly as possible in order to minimize the effect of space charge and consequently keep emittance growth to a minimum.

3 Simulations

A number of simulations were undertaken to examine the performance of the extraction system of the ion source. Initially, 2D electrostatic modeling of the source plate, extraction electrode, and ground electrode were performed using the free software Finite Element Method Magnetics (FEMM) 4.2 [3]. The geometries in FEMM were created with the help

of version 4 of the built-in, C-like Lua scripting language. The main advantage was that the dimensions of the extraction and ground electrodes could be input directly into the script, which would then automatically perform the necessary trigonometric calculations to create the requested geometry. However, the first simulations only worked well for relatively large mesh sizes, resulting in a coarse representation of the electric potential lines; this was found to be due to meshing the electrodes when they should not have been meshed. Despite this, there was an indication that increasing the cone angle of the extraction electrode might lead to an improvement of beam emittance; the beam would spend less time inside the cone where the electric field was very low and consequently suffer less space charge effects.

3.1 SIMION

The SIMION 8.0 software [2] was recommended by Cheng-Yang Tan as an all-in-one geometry modeler and particle tracking program. Though SIMION allows the use of constructive solid geometry operations to directly create 3D structures, 2D geometry construction proved to be necessary to obtain features like rounded or broken edges. The 2D geometry was subsequently rotated around the x-axis to obtain an axisymmetric model. Initially, the plan was to model the hydrogen plasma itself behind the source plate, so as to have an accurate model of the ion source. This approach had to be modified when it became clear that SIMION cannot accurately model particle beams in high space charge regions; in fact, page 8-18 of the SIMION manual states: “Beware, this approach [of using a small group of ions] doesn’t model the space charge effects in ion source regions.”

Though the ion source simulations were not at all accurate with regard to final emittance or efficiency of execution (only 1 out of every 100 particles was successfully extracted and tracked through the geometry), they did predict the presence of a very small waist approximately midway between the source plate and the extraction electrode. This was confirmed by observing the 750 kV Cockcroft-Walton ion sources utilized by Fermilab and by divergence measurements made by Chuck Schmidt; in both cases, the beam passed

through a small waist just after exiting the source box. Based on this result, subsequent simulations were begun at this waist so as to avoid the limitations of SIMION's simulation of ion sources.

SIMION includes an interpreter for the Lua scripting language as well, allowing nearly all aspects of the simulation, including the geometry, to be controlled from several script files. A master program, `simhins`, was written in C to control SIMION from the command line and allow easy modification of quantities such as the extraction voltage and the beam current, while a Lua script running with the simulation itself collected the output. The geometry generation commands and the ion definitions are stored in separate files. As in the FEMM simulations, the geometry was created with the help of Lua commands, and the electrostatic lens was added to the extraction geometry at this point. Note that because this 2D geometry is later rotated around the x-axis, the longitudinal axis in the SIMION simulations is x, rather than z, as is the convention. The ions to be simulated were set up using SIMION's `.fly2` file format. A uniformly distributed circular emission area was used, with radius and position equal to that of the waist, and the particles were given initial energies from a Gaussian distribution centered around the average energy of the particles at the waist. The simulation parameters are summarized in Table 1.

At first, the emittance of the simulated beam was computed by binning the positions and velocities of the particles to produce an intensity versus position-and-velocity plot much like those obtained from an emittance scanner. The main issue with this approach is that low number of particles cause the intensity plot to have holes, even in the beam core; these holes move around from simulation to simulation since the starting positions and energies of the particles are set by distributions. Larger bin sizes eliminated the holes but reduced the resolution of the plots. RMS emittance was chosen as a more reliable way of comparing the final emittances, since it is easily calculated for discrete particles [Eqn. 2]. At the end of a simulation (or even during the simulation), the Lua script dumps all information about the ions into a text file, which is processed using an Octave/MATLAB function, `gpemit`,

that performs the RMS emittance calculation.

One main limitation encountered while using SIMION to construct the simulation geometry was an apparent fundamental minimum resolution of 1x1x1 mm cubes for its potential grid. Since the lengths and distances in the extraction geometry are on the order of 1 mm, the result gives non-smooth and incorrectly sized electrodes. The cone of the extraction electrode must be approximated with 1 mm cubes, leading to an aperture that is not representative of the actual geometry. Therefore, the effect of changing the extraction aperture was not accurately modeled using SIMION. There is an indication, however, that this limitation can be overcome by generating larger than actual geometry and then scaling it down within SIMION, which would increase the resolution of the resulting grid. An alternate method is currently being investigated, in which the electric field computations are performed by FEMM (which uses vector-based geometry) to arbitrary resolution, and then imported into SIMION for particle tracking and visualization.

4 Results

The initial electric field simulations using FEMM are found in Figure 12. Of all the parameters, the extraction gap had the largest effect on the final emittance of the beam. Figure 1 shows two different simulations conducted with 2,000 particles each; the cone angle and aperture have been held constant while the gap and extraction voltage have been increased for the second simulation [Fig. 1b]. A larger aperture size also led to decreased emittance, though the effect was smaller by a factor of at least 5 [Fig. 3]. In the SIMION simulations, changing the cone angle provided limited or no benefit, though this is thought to be due in part to the minimum resolution of the SIMION geometry generator as discussed above. Additionally, the original motivation for increasing the cone angle was to allow the electric field to penetrate deeper into the cone so as to decrease the time the beam spent in a region of low acceleration. However, increasing the cone angle also

decreases the curvature of the equipotential surfaces inside and behind the cone, leading to less focusing during the acceleration gap between the extraction and ground electrodes. This effect may explain the relatively poor performance of the 60 degree cone as compared to the 45 degree cone [Fig. 2].

A comparison between the 45 degree cone, 2 mm aperture, 2 mm gap, and 13.5 kV extraction voltage configuration and the final 45 degree cone, 3 mm aperture, 4 mm gap and 25 kV extraction voltage using 5,000 particles shows a remarkable decrease in simulated final emittance [Fig. 5] and real final emittance [Fig. 4]. The mechanism for this decrease in emittance is thought to be primarily due to reduced space charge effects. Since the beam reaches a higher energy before passing into the low-field region inside the extraction electrode cone, special relativity causes the beam to be stiffer with respect to charge repulsion inside the beam. The beam current also increased to above 24 mA of H^- , compared to only 21.8 mA of H^- for the previous configuration.

Emittance scans from the ion source and simulation results both showed a final beam with S-shaped tails in phase space [Fig. 13]. Since the beam nearly scrapes on the sides of the electrostatic lens, it was thought that edge effects from the lens were adversely affecting the beam. Divergence measurements with the electrostatic lens off and emittances taken at several locations throughout the simulations further supported this hypothesis. The simulated electrostatic lens was moved upstream, to a position right after that of the ground electrode, and subsequent simulations [Fig. 14] showed that the tails disappeared, although the lens had to be run with a higher voltage in order to achieve the same level of focusing. Given these results, the electrostatic lens was moved 2.54 mm toward the ground electrode in the ion source. The emittance scans in Figure 6 confirm that the tails were eliminated, and show a significant drop in final emittance. This emittance is more characteristic of the future performance of the source when connected to the rest of the HINS linac, since the primary focusing solenoid will be placed close to the ground electrode. SIMION handles space charge using Coulomb's law, which has the additional effect of

causing the number of space charge calculations, and consequently the simulation time, to increase with the square of the number of particles used [Fig. 9]. For a fairly realistic simulation, using at least 2,000 particles was found to be sufficient.

5 Summary

The final emittance and overall beam quality of the HINS ion source testbed was improved by almost a factor of two as a result of increasing the extraction gap and extraction voltage. The effect of changing the cone angle was inconclusive, but increasing the aperture of the extraction electrode did have beneficial effects. SIMION is useful for the purpose of simulating ions flying through the extraction geometry of the source and visualizing the results. However, the issue of minimum grid resolution limits its ability to accurately simulate very small geometries. FEMM is very appropriate for accurate geometry construction and electric field calculations, but cannot track particles. In general, accelerating the beam as quickly as possible will yield the lowest emittances, and edge effects from beam optics cannot be ignored if the beam diameter is close to the inner diameter of the device. Further simulation work using a combination of FEMM and SIMION could be of use in determining the optimal cone angle and aperture size, as well as the effect of further increasing the extraction gap.

6 Acknowledgements

This research was performed at Fermilab as part of the Science Undergraduate Laboratory Internship program under the auspices of the U.S. Department of Energy's Office of Science. The author gratefully acknowledges the guidance and teaching of mentors Raymond Tomlin and Charles Schmidt, as well as the emittance measurements by Doug Frome, and the contributions of Cheng-Yang Tan and Jean-Francois Ostiguy.

References

- [1] R. C. Webber et al., “Overview of the High Intensity Neutrino Source Linac R&D Program at Fermilab,” 2008, Presented at 24th International Linear Accelerator Conference (LINAC08), Victoria, British Columbia, Canada, Sept. 29–Oct. 3 2008.
- [2] Scientific Instrument Services, Inc., “SIMION 8.0,” <http://simion.com>.
- [3] D. C. Meeker, “Finite Element Method Magnetics, Version 4.2 (01Apr2009 Build),” <http://femm.foster-miller.net>.
- [4] D. P. Moehs, J. Peters, and J. Sherman, “Negative hydrogen ion sources for accelerators,” *Plasma Science, IEEE Transactions on* 33, 6: (2005) 17861798.
- [5] M. P. Stockli, “Measuring and Analyzing the Transverse Emittance of Charged Particle Beams,” In Beam Instrumentation Workshop 2006, T. S. Meyer and R. Webber, Eds. AIP, 2006, volume 868, 2562, <http://link.aip.org/link/?APC/868/25/1>.
- [6] H. Zhang, *Ion Sources*, Springer-Verlag, 1999.

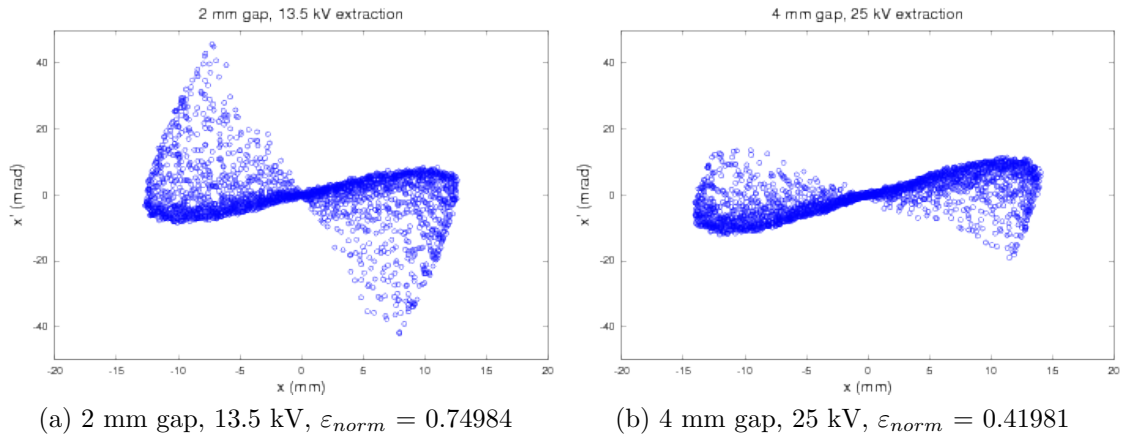


Figure 1: Effect of increased extraction gap (simulation); both simulations use 45 degree cone angle and 2 mm aperture.

parameter	typical value	parameter	typical value
extraction voltage	-38 kV to -25 kV	high voltage	-50 kV
cone angle	30 degrees to 60 degrees	initial position	3 mm
gap	2 mm to 4 mm	initial radius	0.5 mm
aperture	2 mm to 4 mm	E_{ave}	6000 eV
		E_{FWHM}	100 eV
		half angle	1.5 degrees

(a) Varied parameters

(b) Constant parameters

Table 1: Parameters for the SIMION simulations as well as their typical values.

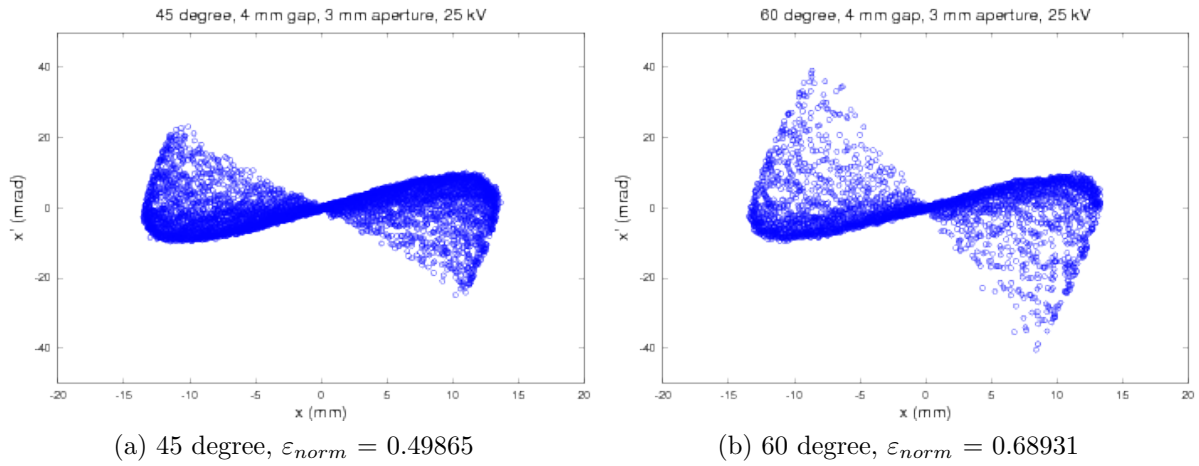


Figure 2: Effect of cone angle (simulation); both simulations use 4 mm gap, 3 mm aperture, and 25 kV extraction voltage.)

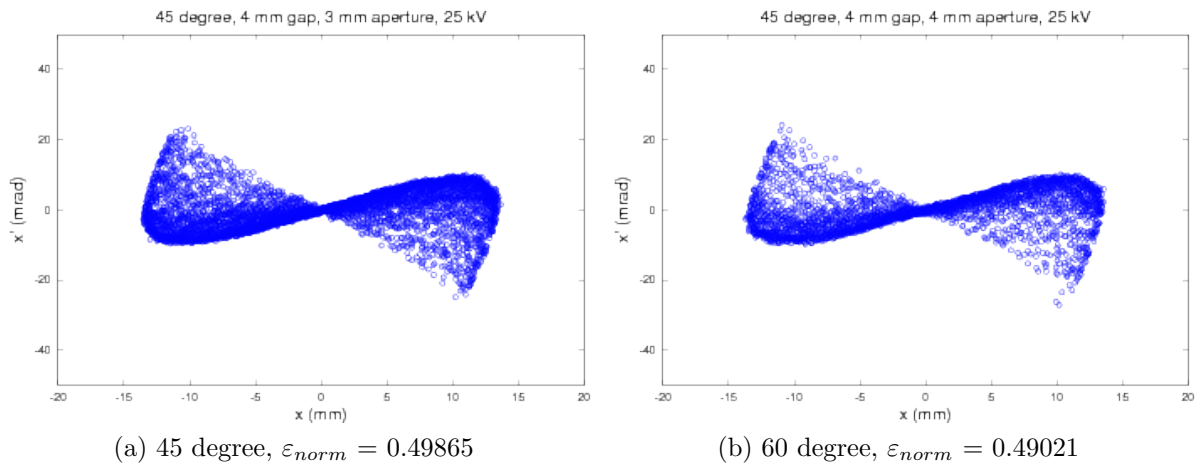
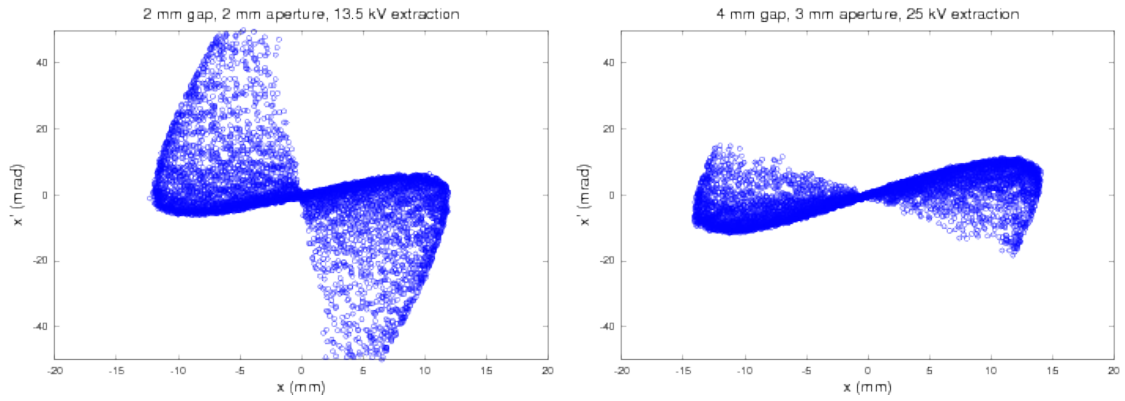
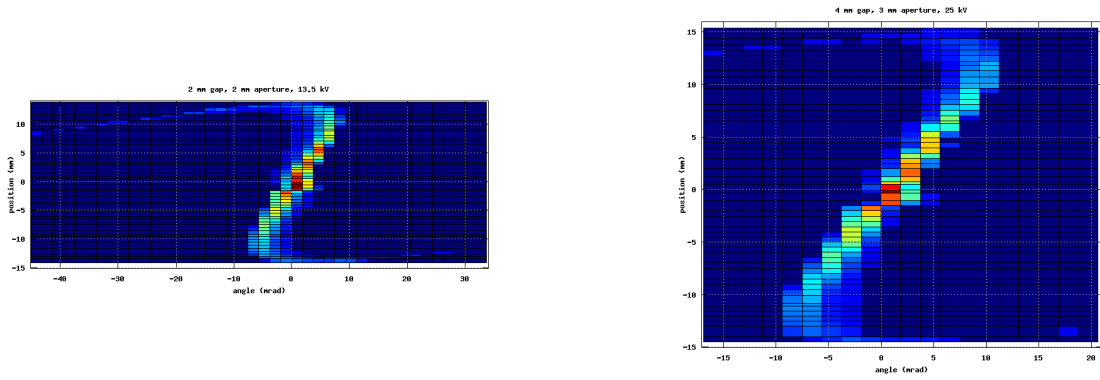


Figure 3: Effect of extraction aperture (simulation); both simulations use 45 degree cone angle, 4 mm gap, and 25 kV extraction voltage.)



(a) 30 degree, 2 mm gap, 2 mm aperture, 13.5 kV extraction, $\epsilon_{norm} = 1.1047$ (b) 45 degree, 4 mm gap, 3 mm aperture, 25 kV extraction, $\epsilon_{norm} = 0.41880$

Figure 4: Comparison of 45 degree extraction geometries (simulations).



(a) 30 degree, 2 mm gap, 2 mm aperture, 13.5 kV extraction, $\epsilon_{norm} = 0.859771$ (b) 45 degree, 4 mm gap, 3 mm aperture, 25 kV extraction, $\epsilon_{norm} = 0.667734$

Figure 5: Comparison of 45 degree extraction geometries (actual).

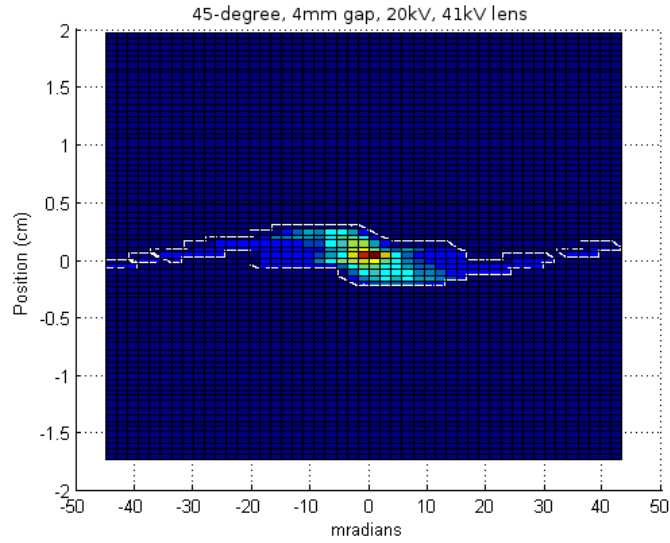
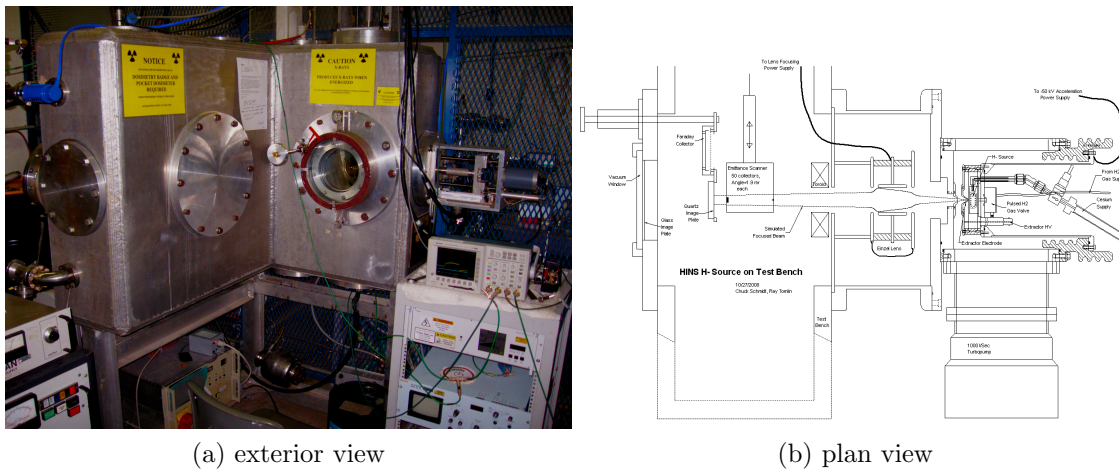


Figure 6: 45 degree, 4 mm gap, 3 mm aperture, 20 kV extraction, with moved lens; $\epsilon_{norm} = 0.5471$.



(a) exterior view

(b) plan view

Figure 7: HINS ion source in testbed.

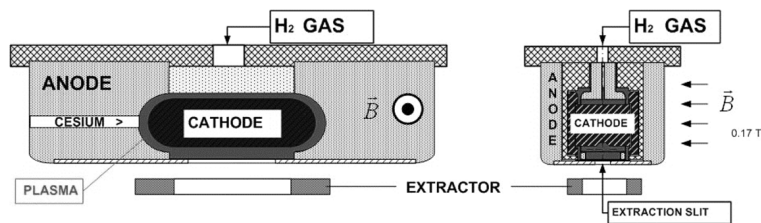


Figure 8: Diagram of magnetron ion source [4]; in the case of HINS, the aperture to the source is circular rather than rectangular as shown.

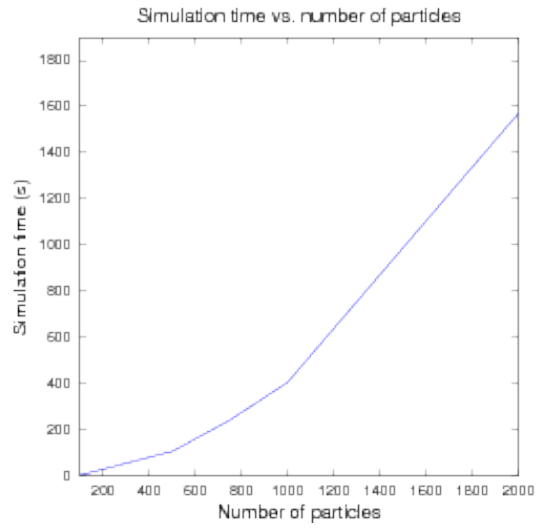


Figure 9: Plot of simulation time versus the number of particles in the simulation.



Figure 10: Current location of HINS linac in Fermilab's Meson Detector Building.

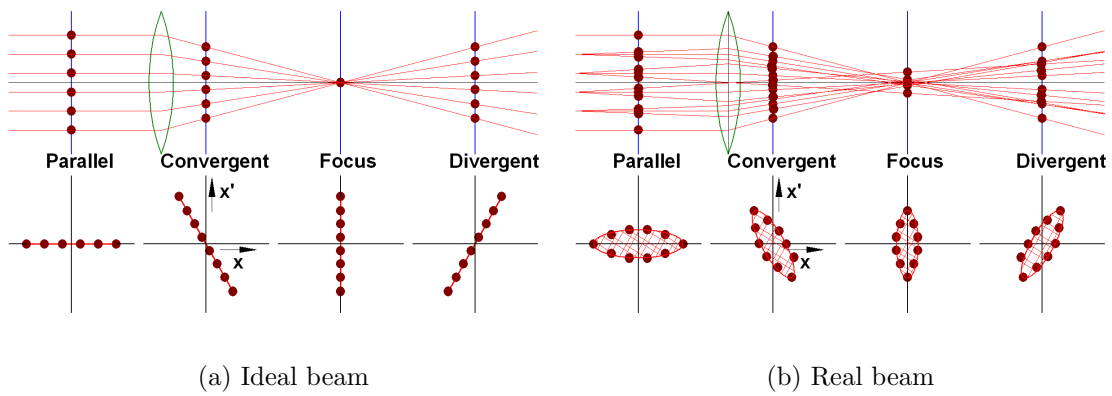
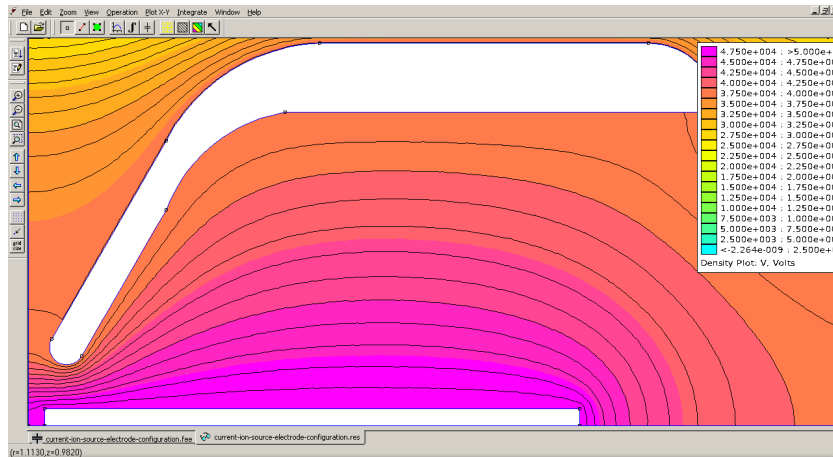
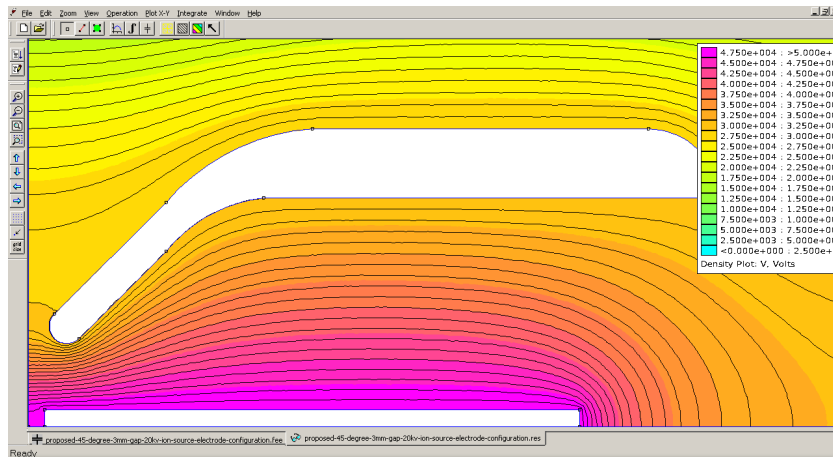


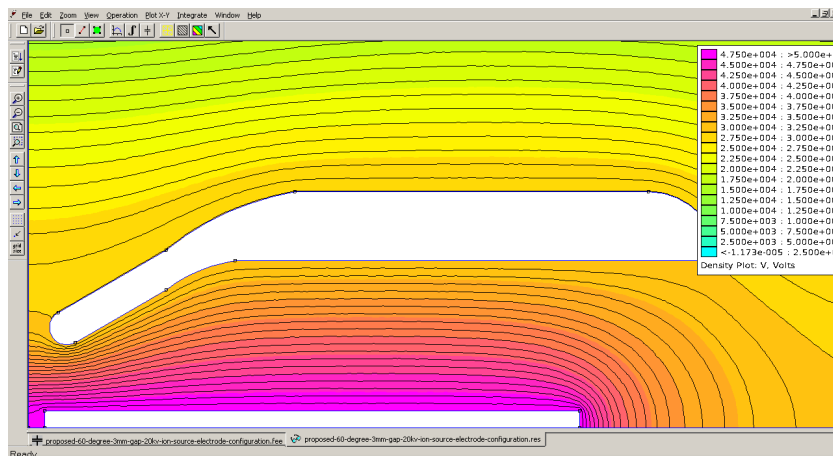
Figure 11: Transformation of emittance during focusing.



(a) 2 mm gap, 2 mm aperture, 30 degree cone, 12 kV

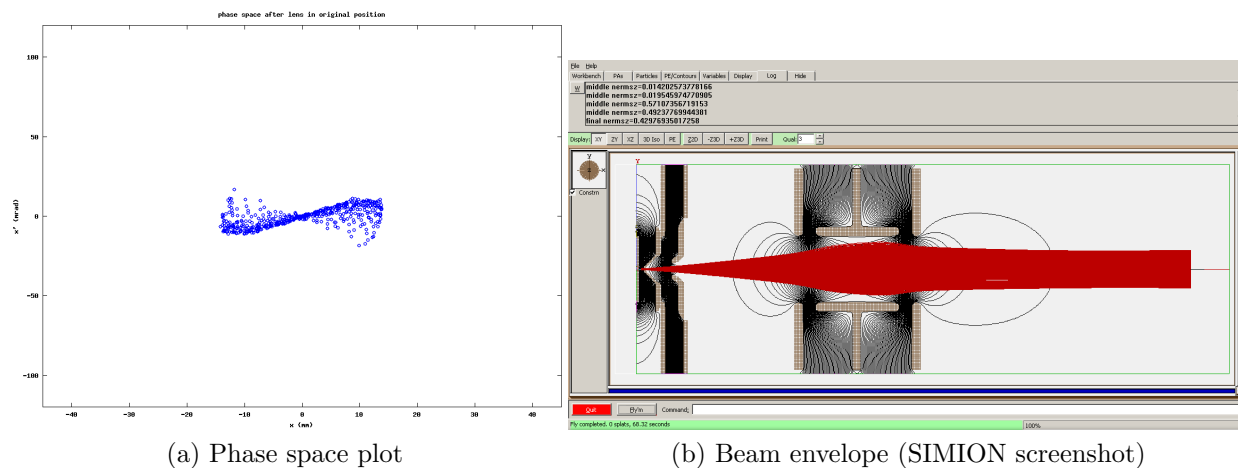


(b) 3 mm gap, 2 mm aperture, 45 degree cone, 20 kV



(c) 3 mm gap, 2 mm aperture, 60 degree cone, 20 kV

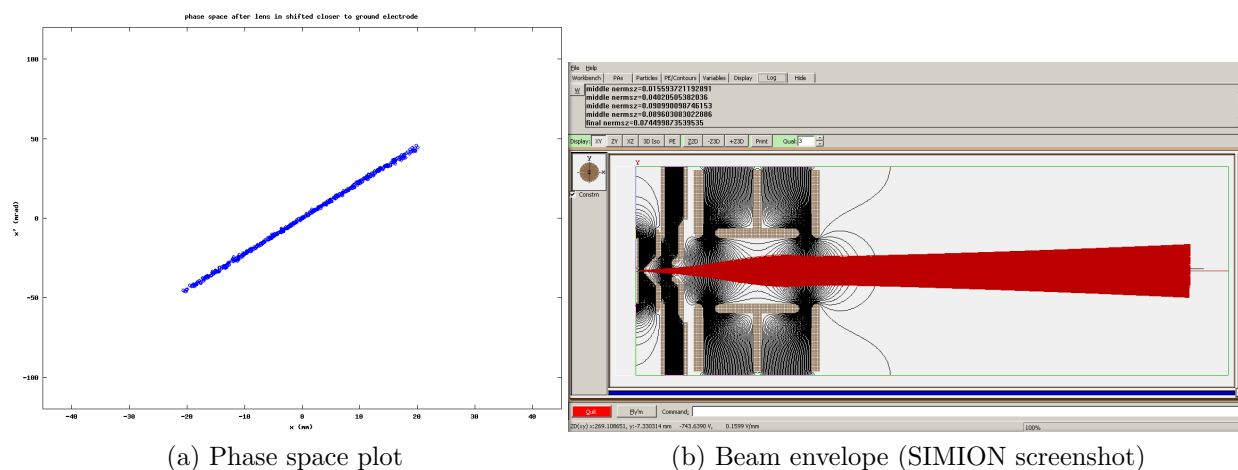
Figure 12: Initial FEMM electric field simulations.



(a) Phase space plot

(b) Beam envelope (SIMION screenshot)

Figure 13: Electrostatic lens in original position.



(a) Phase space plot

(b) Beam envelope (SIMION screenshot)

Figure 14: Electrostatic lens shifted very close to ground electrode.